

MULTIPLE TECHNIQUES AT GRAZ SLR STATION FOR THE CHARACTERIZATION OF SPACE DEBRIS

Michael A. Steindorfer⁽¹⁾, Franz Koidl⁽¹⁾, Sebastian Schneider⁽¹⁾, Nadine Trummer⁽¹⁾, Peiyuan Wang⁽¹⁾, Georg Kirchner⁽¹⁾

⁽¹⁾Space Research Institute, Austrian Academy of Sciences, Schmiedlstraße 6, A-8042 Graz, Austria, Email: michael.steindorfer@oeaw.ac.at

ABSTRACT

Attitude determination of space objects ideally relies on multiple techniques to characterize its behaviour in orbit. Within this paper different measurement and simulation techniques used at Graz SLR station are presented. Satellite laser ranging (SLR) precisely measures the range to targets equipped with corner cube retro reflectors (CCRs). Using higher power lasers allows to detect diffusely reflected photons of space debris as well. Laser ranging data is simulated to CCRs or space debris objects with arbitrary orientation in space. Simultaneously to SLR single photon light curves are recorded by detecting reflected sunlight from space objects. An outlook towards future MHz SLR concludes the paper.

1 GRAZ SLR STATION

Since 1982 Graz SLR station is performing precise range measurements [1, 2] to different targets from low Earth up to geostationary orbit. Over the centuries the precision was continuously improved upgrading laser, detector and calibration technology. Currently, a 10 ps laser operating at 2 kHz with 0.8 W, a compensated single photon avalanche detector [3] and highly accurate event timers reduced single shot precision to 2-3 mm. For space debris laser ranging [4, 5] a higher powered laser with 16 W with a pulse width of 3 ns is used to measure diffusely reflected photons from space debris objects. Since 2015, the reflected sunlight from space objects is measured using a single photon detector [6], allowing a temporal resolution down to microseconds. Optical image analysis tools allow for the detection of satellites and space debris for improved alignment and for pointing determination based on plate solving [7]. In addition to range and light curve measurements, simulations of laser ranging data are conducted [8]. Utilizing the SLR measurements and satellites with known orientation, simulations can be verified accordingly.

2 SATELLITE LASER RANGING

The analysis of laser ranging data requires a few post processing steps to remove noise and orbital inaccuracies. Observed-minus-calculated residuals are calculated, which represent the difference of the

predicted range to the measured range. As the raw dataset is calculated w.r.t. the inaccurate orbit a slope in the data set is visible (Fig. 1). Improving the orbit based on the measured dataset, reveals fine details within the data. Jason-2 is rotating and range variations in the residuals show its apparent rotation period (Fig. 2). The CCRs are always pointing towards the observer, allowing first conclusions on the attitude.

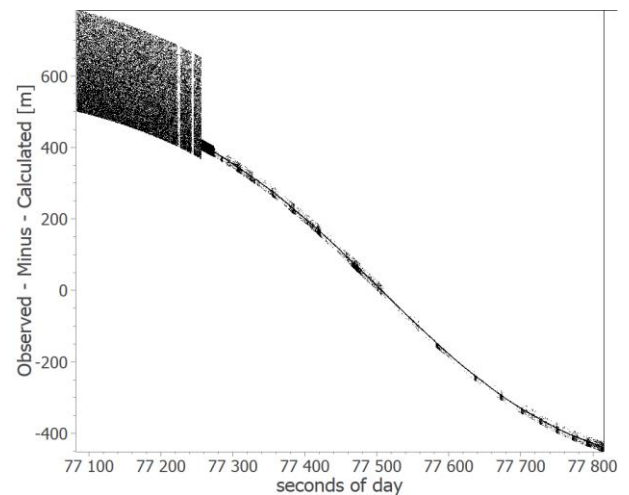


Figure 1. Raw SLR Observed-Minus Calculated residual data to the defunct satellite Jason-2.

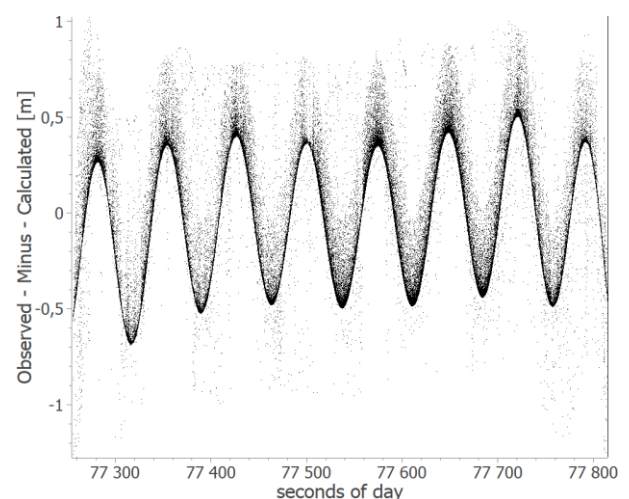


Figure 2. Orbit cleaned SLR residuals revealing the rotation of Jason-2 based on range variations.

Zooming in even further and fitting through the data even allows to identify single CCR of the pyramid moving in and out (Fig. 3). The fit corresponds to a movement of the CCR around the optical center of the pyramid.

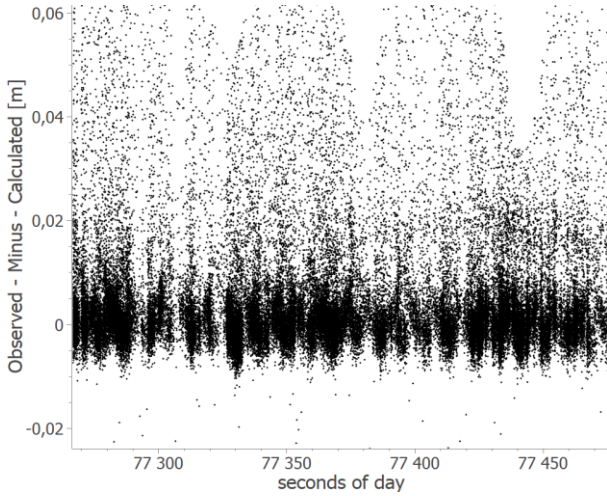


Figure 3. Fitted SLR observed minus calculated residual data to defunct satellite Jason-2 showing the individual CCRs.

SLR residuals can be simulated if the arrangement of the CCRs and the attitude of the object in orbit is known. An arbitrary rotation axis can be defined, allowing for a given rotation with respect to a reference coordinate frame. From the provided dataset attitude determination algorithms can be tested and validated w.r.t. known conditions. Furthermore, the placement of CCRs on the satellite can be planned assisting future removal missions.

For a Low Earth Orbit (LEO) pass (e.g. Technosat) the SLR residuals (Fig. 4) are calculated assuming a box-type satellite with 1-4 CCRs on each side (Fig. 5) placed approx. 1 meter apart. The rotation axis is assumed to be pointing through the face A1 and A3 with a period of 180 seconds. The CCRs of the individual sides are color-coded to allow easier identification. Assuming single photon sensitivity and a single shot precision of 2-3 mm, the individual tracks of the satellite will be easily identifiable. In addition to that based on the sequence and number of CCRs visible at the same time, conclusions on the rotation direction can be drawn.

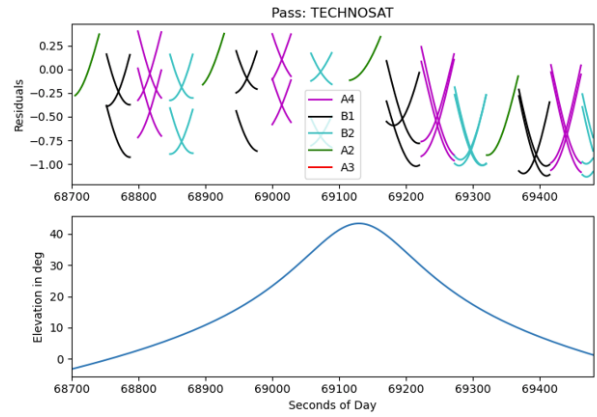


Figure 4. Raw satellite laser ranging observed minus calculated residual data to defunct satellite Jason-2.

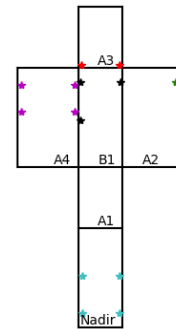


Figure 5. Arrangement of 1-4 CCRs on a box-type satellite leading to the above pattern of residuals.

3 SPACE DEBRIS LASER RANGING

Utilizing a higher power laser, the diffuse reflection of space objects can be detected. Due to the low amount of photons scattered towards the observer, SDLR is operating in the single photon regime. Hence, the photons from the whole body can be detected, depending on the orientation, from ranges varying according to the size of the object. Based on a measurement to the rotating defunct satellite Envisat (Fig. 6) the difference between satellite laser ranging and space debris laser ranging becomes obvious. At the beginning of the pass (up to second 14000) returns from a very narrow range region are visible - the CCRs reflect a very large number of photons and the detector only measures ranges from the CCRs. Later on throughout the pass, the CCRs turn away from the field of view of the observing station and the photons are reflected from the whole body. If the reflected photons come from a narrow range region the satellite is oriented perpendicular to line of sight, showing the station only a short depth information. Once the satellite has continued its rotation the satellite body is oriented close to the line of sight and large depth information of up to 20 meters is found.

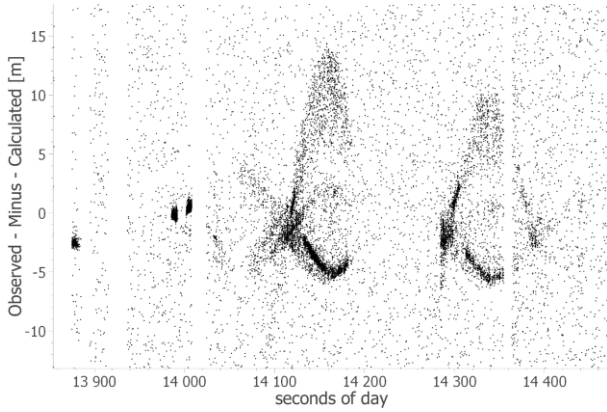


Figure 6. Space debris laser results coming from CCRs and diffuse reflection while ranging to Envisat.

Space debris laser ranging residuals can also be simulated. A grid of 700 points is created based on a simple model of an upper stage rocket body with a nozzle and an overall height of 16 meters (Fig. 7).

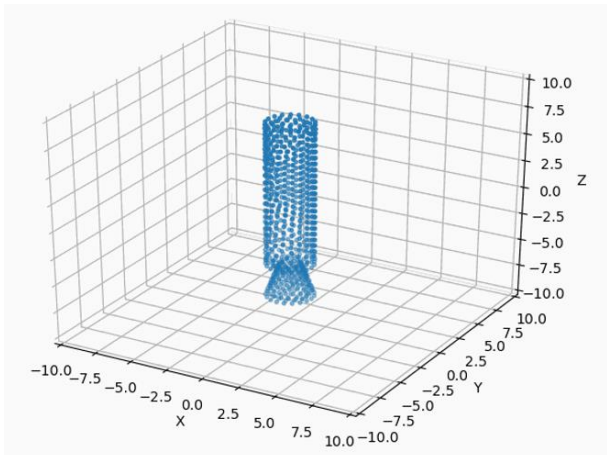


Figure 7. A simple 3D grid model of an upper stage rocket body.

Based on these points residuals are simulated for different rotation axes: $[1, 0, 0]$ and $[0, 0, 1]$.

In the first case for rotation axis $[1, 0, 0]$ for the simulated pass a rotation is found similar to the previous case of Envisat (Fig. 8). The body is repeatedly facing towards the observer and aligned perpendicular to the observer. The denser pattern within the residuals comes from the nozzle, as all mesh points are used to simulate the data. In reality the nozzle will block potential returns from the inner part.

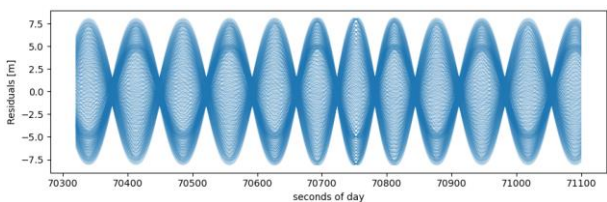


Figure 8. SLR residuals of a rotation around $[1,0,0]$ axis.

Applying a center of mass offset of 1 meter reveals an additional periodical shift of the pattern (Fig. 9) which could be used to identify the different sides of the body.

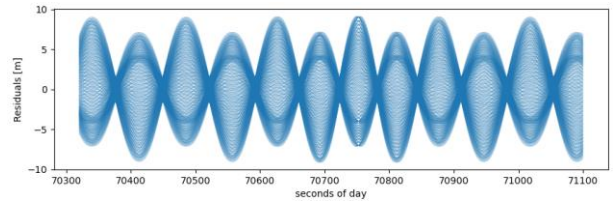


Figure 9. SLR residuals of a rotation around $[1,0,0]$ axis with a center of mass offset along the z-axis of 1 meter.

Due to the z-axial symmetry a rotation around the $[0, 0, 1]$ axis (Fig. 10) removes any rotation effect from the data and the difference in range purely comes from the apparent movement of the object along the orbit. Again the denser-meshed region corresponding to the nozzle is visible.

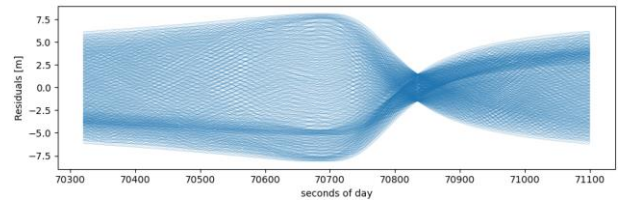


Figure 10. SLR residuals of a rotation around $[0,0,1]$ axis show only range variation due to the apparent motion of the object above the observer.

4 SINGLE PHOTON LIGHT CURVES

Data fusion of single photon light curves and space debris laser ranging data potentially gives additional insight on the rotational behavior of space objects. Reflections of specific surfaces can be correlated to the residuals. The rotation of a re-entering upper stage rocket body reveals a correlation of the light curve with the SLR residuals. At minimal residuals a broad intense peak can be found which is coming from the cylindrical surface. As the rotation continues maximal residuals correlate to a reflection from the top/bottom surface. Furthermore, the center of mass offset can be detected similar to the simulations in Fig. 9.

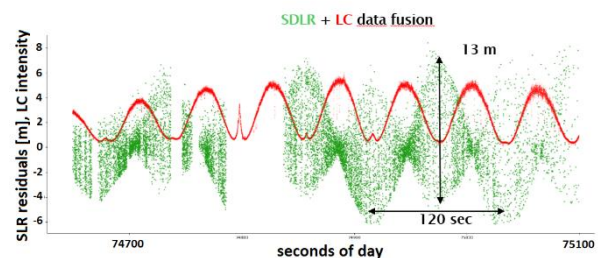


Figure 11. Simultaneous space debris laser ranging and single photon light curve measurement to an upper stage rocket body.

5 MEGAHERTZ SLR

In the future in the SLR community we expect an ongoing trend pushing towards higher repetition rates [9, 10, 11]. In 2021 and 2022 Graz conducted first experiments with a picosecond laser with repetition rate up to 1 MHz. For that a burst mode operation had to be realized to avoid backscatter overflow of the detector. Furthermore, a new “propagated range gate” technique is shown, avoiding to push the limits of FPGA operation.

It was found that it is possible to increase the data rate to LEO satellites up 260,000 returns/sec - equivalent to an increase by a factor of 150. For geostationary or GNSS target an increase of a factor of 10 was seen (Fig. 12).

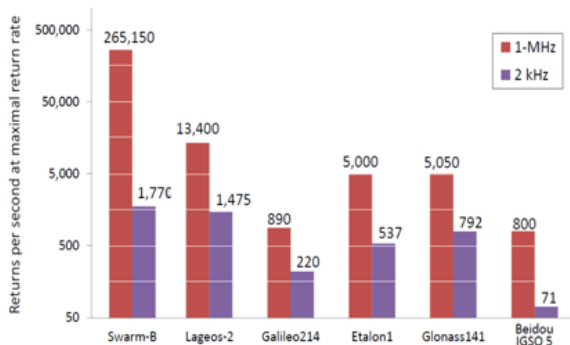


Figure 12. MHz SLR statistic at Graz SLR station.

The satellite signature of various satellites could be identified showing that increased returns per second while the single pulse returns are strictly at single photon level has significant advantages (Lares-2, Fig. 13).

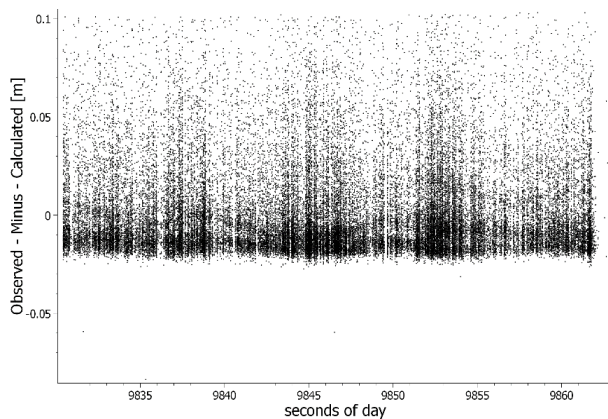


Figure 13. MHz satellite signature of Lares-2 measured at Graz SLR station.

6 REFERENCES

1. Degnan, J. J. (1993). Millimeter accuracy satellite laser ranging: A review. *Geodynamics Series* (eds. Smith, D. E. & Turcotte, D. L.) 25, 133–162
2. Pearlman, M. R., et al. (2002). The International Laser Ranging Service. *Adv. Space Res.* 30, 135–143.

3. Kirchner, G., et al. (1999). SPAD time Walk Compensation and Return Energy Dependent Ranging. 11th International Workshop on Laser Ranging.
4. Sproll, F. et al. (2016). Two-color and multistatic space debris laser tracking. 20th International Workshop on Laser Ranging.
5. Steindorfer, M. A. et al. (2020). Daylight space debris laser ranging. *Nat Commun.* 11, 3735.
6. Steindorfer, M. A. et al. (2015). Light Curve Measurements with Single Photon Counters at Graz SLR, Technical Workshop on Laser Ranging.
7. Steindorfer, M. A. et al. (2017) Stare and chase of space debris targets using real-time derived pointing data. *Adv. Space Res.* 60, 1201–1209.
8. Steindorfer, M. A. et al. (2022) Reflector-Based Attitude Detection System. 73rd International Astronautical Congress (IAC)
9. Wang, P. et al. (2021). Megahertz repetition rate satellite laser ranging demonstration at Graz observatory. *Opt. Lett.* 46, 937
10. Dequal, D. et al. (2021) 100 kHz satellite laser ranging demonstration at Matera Laser Ranging Observatory. *J. Geod.* 95, 26.
11. Long, M. et al. (2022) Satellite laser ranging at ultra-high PRF of hundreds of kilohertz all day. *Front. in Phys.* 10